

Entanglement properties and quantum phases for a fermionic disordered one dimensional wire with attractive interactions

Richard Berkovits

Department of Physics, Jack and Pearl Resnick Institute, Bar-Ilan University, Ramat-Gan 52900, Israel

A fermionic disordered one dimensional wire in the presence of attractive interactions is known to have two distinct phases: A localized and a superconducting one depending on the strength of interaction and disorder. The localized region may also exhibit a metallic behavior if the system size is shorter than the localization length. Here we show that the superconducting phase has a distinct distribution of the entanglement entropy and entanglement spectrum distinct from the metallic regime. The entanglement entropy distribution is strongly asymmetric with Lévy alpha stable distribution (compared to the Gaussian metallic distribution), and the entanglement level spacing distribution is unitary (compared to orthogonal). Thus, entanglement properties may reveal properties which can not be detected by other methods.

PACS numbers: 73.20.Fz, 03.65.Ud, 71.10.Pm, 73.21.Hb

In the last decade the application of concepts from quantum information, such as entanglement entropy (EE)[1], took center stage in understanding physical phenomena in condensed matter physics. One of the reasons for this interests is that EE is deeply connected to quantum phase transitions (QPT). The EE quantifies the entanglement in a many-body system by dividing it into two regions A and B. For a system in a pure state $|\Psi\rangle$, the entanglement between regions A and B is measured by the EE $S_{A/B}$ connected to the eigenvalues of the reduced density matrix of area A, ρ_A or B, ρ_B . It is expected that non-local properties, such as the EE, may provide a different perspective beyond the traditional point-point correlations and local order parameters [2].

Specifically, ρ_A is defined as: $\rho_A = \text{Tr}_B |\Psi\rangle\langle\Psi|$, where the degrees of freedom of region B are traced out. The eigenvalues of the matrix λ_i^A are used to calculate the EE:

$$S_A = - \sum_i \lambda_i^A \ln \lambda_i^A. \quad (1)$$

Recently it has been understood that one can utilize the information enclosed in the full spectrum of $\{\lambda_i^A\}$. These eigenvalues are used to construct the entanglement spectrum (ES) $\{\varepsilon_i^A = -\ln \lambda_i^A\}$ [3]. For one-dimensional (1D) systems, the area of the boundary between regions A and B is fixed and thus the EE should not depend on the size of region A. Nevertheless a logarithmic dependence of the form [4–7]:

$$S(L_A, L) = \frac{1}{6} \ln \left(\sin \left(\frac{\pi L_A}{L} \right) \right) + c, \quad (2)$$

where L_A is the length of region A and L is the samples length, is expected in the metallic (clean) regime. Several years ago Li and Haldane [3] came up with an intriguing conjecture regarding the connection between the ES and the excitation spectrum of a many-body state. They suggested that the low-energy ES shows a precise correspondence to the true many-particle spectrum of region

A. The properties of the EE and the ES may be used to identify phase transitions in disordered many-body properties [8–16].

In this letter we will use the EE and ES in order to investigate the nature of different phases of fermionic disordered 1D systems with attractive interactions. Electron-electron interactions in 1D systems are parametrized by the Luttinger parameter K [17, 18]. For non-interacting systems $K = 1$, while for attractive interactions $K > 1$. When both disorder and interaction are present, an extended metallic (with superconducting correlations) phase is expected once attractive interactions are strong enough, i.e. $K > 1.5$ [18–21]. This stems from the renormalization group scaling of the localization length

$$\xi = (\xi_0)^{1/(3-2K)}, \quad (3)$$

where ξ_0 is the non interacting localization length. Thus, for $K = 1.5$ the localization length diverges, and one transits from the localized to the extended regime. Indeed, it has been numerically demonstrated that with strong enough attractive interactions in the usual Anderson model [13, 22–24] metal-like behavior emerges, although no evidence of superconducting correlation have been numerically demonstrated.

For disordered system one must consider the EE behavior over an ensemble of different realizations of disorder. It has been demonstrated in Ref. [11] that the median EE for $L_A < \xi$ follows the metallic logarithmic behavior (Eq. (2)), while for $L_A > \xi$ it saturates. In principal this could be used to decide in what phase (localized or metallic) the system is in [13]. Nevertheless, in a realistic numerical study this strategy is fraught with problems, since the localization length grows fast as function of K (Eq. (3)), and easily outgrows any finite system length L . Once $\xi \gg L$ a finite system will show metallic behavior although it is in the localized regime. For brevity, we shall refer to the $K > 1.5$ regime as superconducting, and to the finite sample $K < 1.5$ regime

as localized or metallic according to whether $L > \xi$ or $\xi > L$.

In this Letter we will show that the full distribution of the EE shows a distinct behavior between the metallic and superconducting regime, although the median EE is essentially identical in both regimes. The EE distribution changes from a Gaussian in the metallic regime to a very asymmetric Lévy alpha stable distribution with “fat tails” in the superconducting regime. The ES level spacing (ESLS) distribution fits the Gaussian orthogonal distribution (GOE) expected from interacting many particle system [8, 9, 25–30] in the metallic regime, while it changes to a Gaussian unitary distribution (GUE) associated with superconducting excitations [31, 32] in the superconducting regime. Thus, the EE and ESLS distributions are able to characterize the phase of the system, where other methods fail.

In this letter we consider a spinless 1D electrons wire of size L with *attractive* nearest neighbor interactions and on-site disordered potential. The system’s Hamiltonian is given by:

$$H = \sum_{j=1}^L \epsilon_j \hat{c}_j^\dagger \hat{c}_j - t \sum_{j=1}^{L-1} (\hat{c}_j^\dagger \hat{c}_{j+1} + h.c.) \quad (4)$$

$$+ U \sum_{j=1}^{L-1} (\hat{c}_j^\dagger \hat{c}_j - \frac{1}{2})(\hat{c}_{j+1}^\dagger \hat{c}_{j+1} - \frac{1}{2}),$$

where ϵ_j is the on-site energy, which is drawn from a uniform distribution $[-W/2, W/2]$, \hat{c}_j^\dagger is the creation operator of a spinless electron at site j , and $t = 1$ is the hopping matrix element. The interaction strength is $U < 0$, and a background is included. For the non-interacting Anderson model the system is localized with a localization length $\xi_0 \approx 105/W^2$ [33]. Here the Luttinger parameter $K(U) = \pi/[2 \cos^{-1}(-U/2)]$ [34, 35]. For non-interacting electrons $K(U = 0) = 1$. For attractive interactions $K > 1$ and ξ increases as U becomes more negative. For $U = -1$, $K = 1.5$ and the localization length according to Eq. (3) diverges. Thus, below $U < -1$ the system is expected to be delocalized. At $U = -2$ it goes through another phase transition to a phase separated state and is insulating again. Indeed numerically [13, 22–24], this system is known to exhibit extended behavior for a range of attractive interaction strength centered around $U = -1.5$ and not too strong disorder $W < 1.5$

The density matrix renormalization group (DMRG) [36, 37]. is a very accurate numerical method for calculating the ground state of disordered interacting 1D system and for the calculation of the reduced density matrix. We calculate the EE for three length $L = 300, 700, 1100$ and different values of $L_A = 10, 20, \dots, L - 10$, for 400, 200, 100 realizations of disorder for the corresponding system length. Specifically, we calculate the normalized EE of the j -th realization at a given L_A , $s_j(L_A) = S_j(L_A)/\langle S(L_A) \rangle$, where $\langle S(L_A) \rangle$ is the average EE over

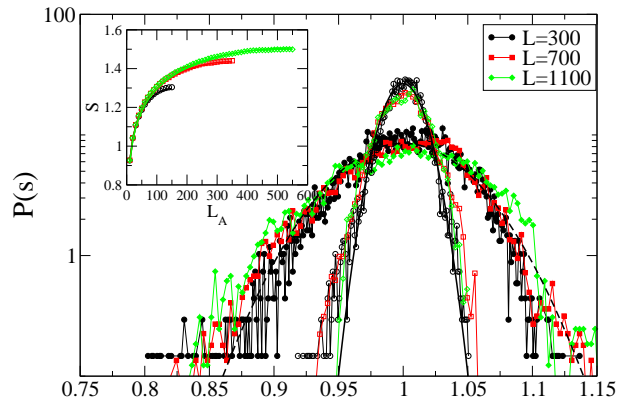


FIG. 1: (Color online) The distribution $P(s)$ of the normalized EE (see text) for different length $L = 300$ (black, circles), $L = 700$ (red, squares), $L = 1100$ (green, diamonds), and disorder strength $W = 0.3$ (empty symbols), $W = 0.7$ (full symbols). A fit to a Gaussian with a width which depends on the disorder, $\sigma(W)$, is depicted by the continuous lines. (inset) The median EE as function of L_A . The symbols correspond to the numerical results, the curves to Eq. (2).

the different realizations. Since the distribution of the EE is very similar for different values of L_A as long as L_A is not too close to the edge we accumulate the distribution of the normalized EE, $P(s)$, in the range of $L/4 < L_A < 3L/4$.

Let us begin by discussing the EE distribution for $U = -0.7$ ($K(U = -0.7) = 1.3$) for which the system is in the metallic regime, i.e., localization length much larger than sample length. In Fig. 1 we present the distribution for two values of disorder ($W = 0.3, W = 0.7$), corresponding to the non-interacting localization length $\xi_0(W = 0.3) \sim 1200$ and $\xi_0(W = 0.7) \sim 200$, thus $\xi(W = 0.3, U = -0.7) \sim 5 \cdot 10^7$, and $\xi(W = 0.7, U = -0.7) \sim 6 \cdot 10^5$. First, we examine the median value of the EE as function of L_A (here we could use the average which is almost equal to the median, but for the sake of uniformity with the upcoming results we use here the median) and compare it with the expression of the EE for a clean system described in Eq. (2). As can be seen in the inset of Fig. 1 it fits quite well. Thus, the median EE follows closely the expected behavior of a clean (metallic) system. The distribution $P(s)$ for all three length and two disorder strength is plotted in Fig. 1. As has been discussed in Ref. [38], for $L \ll \xi$, we expect the distribution to be Gaussian (i.e. $(\sqrt{2\pi}\sigma)^{-1} \exp(-(x-1)^2/2\sigma^2)$) centered at the average. This is indeed seen in Fig. 1 (up to a slight skewness of the tails), as well as the fact that the width, σ of the Gaussian is almost independent of L . On the other hand it is clear that the disorder strength W does affect σ . As might be expected, The weaker is the disorder, the narrower is the width of the Gaussian.

The dependence of the Gaussian width on W is examined in Fig. 2. We keep the length and interaction

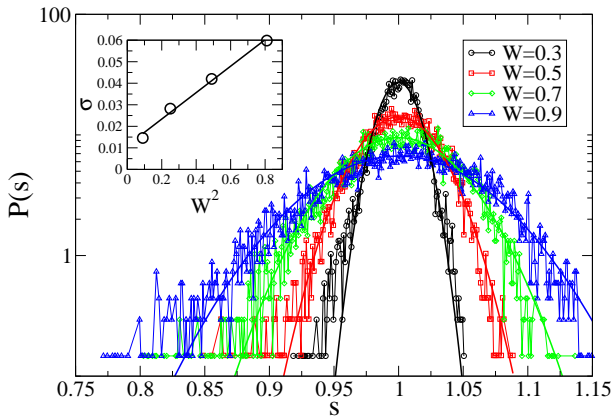


FIG. 2: (Color online) The distribution $P(s)$ of the normalized EE for a fixed wire length ($L = 300$) and different disorder strength: $W = 0.3$ (black circles), $W = 0.5$ (red squares), $W = 0.7$ (green diamonds), $W = 0.9$ (blue triangles). A fit to a Gaussian of width, $\sigma(W)$ (depicted in the inset) is indicated by the continuous lines. (inset) The Gaussian width σ as function of the disordered strength square W^2 .

strength fixed ($L = 300$, $U = -0.7$) while varying W . Even for the strongest disorder $\xi(W = 0.9, U = -0.7) \sim 2 \cdot 10^5$, is much larger than the sample length. $P(s)$ remains Gaussian for all disorder strength. Moreover, as can be seen from the inset $\sigma(W) \propto W^2$.

What happens to the EE distribution in the superconducting regime? Specifically, we concentrate on the extended regime with $U = -1.5$ ($K(U = -1.5) = 2.3$), different values of disorder $W = 0.3, 0.5, 0.7, 0.9$ corresponding to a non-interacting mean free path $\xi_0 \sim 1200, 400, 200, 130$ and different sample length $L = 300, 700, 1100$. This regime of the parameter space is deep in the superconducting regime. We present the distribution $P(s)$ for all length and interaction strength in Fig. 3. It is obvious that $P(s)$ is completely different than in the metallic regime (Figs. 1,2). In all cases the distribution is strongly asymmetric. The typical value of the EE is close to its maximum value, and the probability of measuring an EE larger than the typical value is rather small and falls off abruptly. On the other hand, there is a high probability for measuring values of the EE below the typical value. For smaller values of the EE the distribution has a very long tail. Another difference is the strong dependence on the sample length L even at the same value of disorder W .

First, one concludes that similarly to the case of the EE of a localized system ($L > \xi$) [11, 14, 38], the average EE is not a correct description of the superconducting regime typical EE. The EE is more appropriately represented by the median value. In the inset of Fig. 3 the median value of the EE as function of L_A is compared to Eq. (2). As can be seen it fits quite well.

As can be seen in Fig. 4, the distribution is universal and may be scaled by the function $\tilde{P}(u)$, here

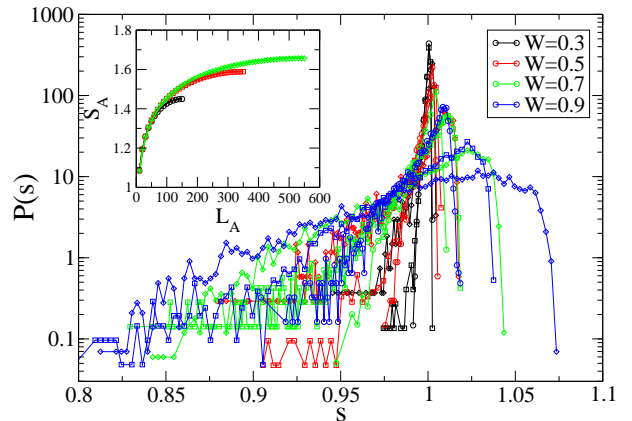


FIG. 3: (Color online) The distribution $P(s)$ of the normalized EE deep in the superconducting regime ($U = -1.5$) for different strength of disorder ($W = 0.3$, black symbols, $W = 0.5$, red symbols, $W = 0.7$, green symbols, $W = 0.9$, blue symbols), and sample length $L = 300$ (circles), $L = 700$ (squares), $L = 1100$ (diamonds). (inset) The median EE as function of L_A . The symbols correspond to the numerical results, the curves to Eq. (2).

$u = 1 + (s - 1) * P_{\max}$, and the distribution is normalized $\tilde{P}(u) = P(u)/P_{\max}$, where P_{\max} is the value of $P(s)$ at the maximum. In the inset of Fig. 4, the values of P_{\max} vs. ξ_0/L is depicted. Up to the ballistic regime, (i.e., for $\xi_0 \gg L$), a linear relation seems to hold. The distribution $\tilde{P}(u)$ may be described rather well by a Lévy alpha stable distribution, which is a natural extension for the central limit theorem to the case that the identically-distributed random variables have no finite variance, and is used to describe distributions with “fat tails”. The Lévy distribution

$$f(x, \alpha, \beta, \gamma, \delta) = \frac{1}{\pi} \text{Re} \int_0^{\infty} e^{it(x-\mu)} e^{-(\gamma t)^{\alpha}(1-i\beta\Phi)} dt, \quad (5)$$

(where $\Phi = \tan(\pi\alpha/2)$, except for $\alpha = 1$ where $\Phi = -(2/\pi) \log(t)$), is defined by four parameters. The stability index $0 \leq \alpha < 2$ characterizes the asymptotic behavior of the tails $|x|^{-1-\alpha}$ (except for $\alpha = 2$), the skewness parameter $-1 \geq \beta \geq 1$, γ is a scale factor and δ controls the location of the maximum [39]. In general f is not analytical, except for special cases, such as $f(x, \alpha = 2, \beta, \gamma = \sigma/\sqrt{2}, \delta = \bar{x})$, equal to a Gaussian of width σ . We plot $f(u, \alpha = 1, \beta = -1, \gamma = 0.285, \delta = 0.8)$, and $f(u, \alpha = 1.2, \beta = -1, \gamma = 0.28, \delta = 0.52)$ in Fig. 4. The skewness is clearly maximal ($\beta = -1$), while fitting α depends very much on the tail region, which has the largest numerical uncertainty. Nevertheless, the main part of the distribution is evidently fitted well by $1 < \alpha < 1.2$.

Thus, although the median of the EE (or its average) does not give us a clear signature whether the system is in the metallic regime or in the superconducting one,

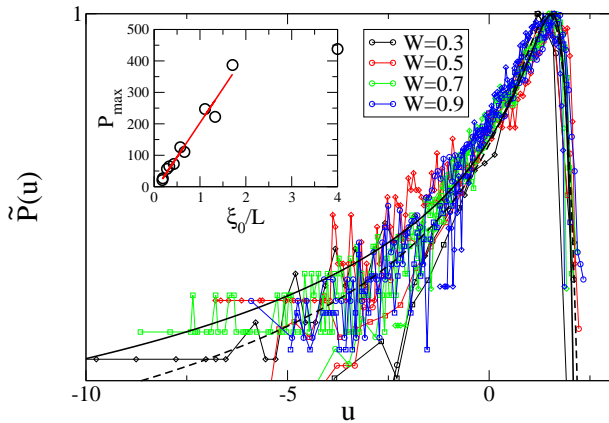


FIG. 4: (Color online) The data presented in Fig. 3 scaled by the parameter u (see text). The continuous (dashed) black curve is the Lévy stable distribution with $\alpha = 1, \beta = -1, \gamma = 0.285, \delta = 0.8$, ($\alpha = 1.2, \beta = -1, \gamma = 0.28, \delta = 0.52$). (inset) The maximum of the distribution $P(s)$ (P_{\max}) depicted in Fig. 3 as function of ξ_0/L . A linear behavior in the regime $\xi_0/L < 2$ is indicated by the line.

the distribution can differentiate between the regimes. Further work is needed in order to follow how the distribution changes as one goes through the phase transition and is the transition point characterized by a special distribution. A hint may be found in Ref. [13], where the variance of the EE is plotted through the transition. It seems that the variance becomes smaller in the metallic side as one approaches the transition and then grows again in the superconducting regime. This is in line with a crossover from a Gaussian distribution to a fat tail one.

In calculating the ESLS one must take into account that different sectors of the reduced density matrix with a fixed number of electrons do not couple with each other. Therefore, for each eigenstate of ρ_A one should calculate both λ_i and N_i^A (the number of particles in the region A). Calculating N_i^A does not add to the complexity of the DMRG code [2]. Thus, each eigenvalue of the reduced density matrix has two indexes $\lambda_i^{N_i^A}$, which are translated into the entanglement Hamiltonian eigenvalues [3] $\varepsilon_i^{N_i^A} = -\ln(\lambda_i^{N_i^A})$. It makes sense to calculate the ESLS only between eigenvalues belonging to the same number sector. Thus, $\Delta_i^{N_i^A} = \varepsilon_{i+1}^{N_i^A} - \varepsilon_i^{N_i^A}$, and $\omega_i^{N_i^A} = \Delta_i^{N_i^A} / \langle \Delta_i^{N_i^A} \rangle$. The average spacing for $U = -0.7$ and $U = -1.5$ for $N_A = L/2 = 350$ as function of i is depicted in the inset of Fig. 5. $\langle \Delta_i^{L/2} \rangle$ only slightly depends on U . There are several anomalously large values appearing for the first few spacings. The distribution $P(\omega)$ is accumulated over all low-lying spacings ($\varepsilon_i^{N_i^A} < 20$), which are not anomalously large (i.e., $\langle \Delta_i^{N_i^A} \rangle < 1$) for all values of N_A , and $L/4 < L_A < 3L/4$. The distributions for the metallic ($U = -0.7$) and superconducting ($U = -1.5$) regimes are presented in Fig. 5. It can be seen that for the metallic case the numerical results fit quite well

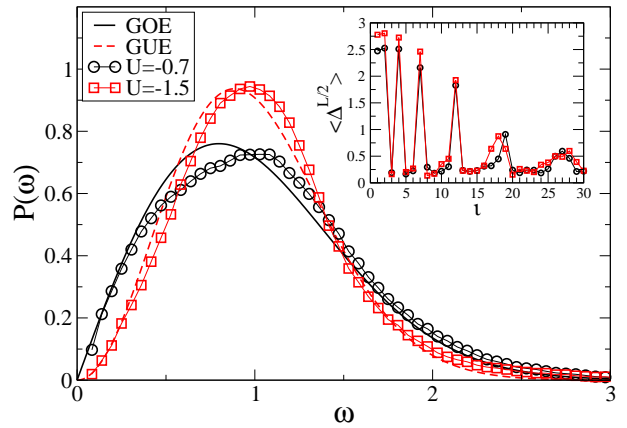


FIG. 5: (Color online) The ESLS distribution $P(\omega)$ as function of the normalized level spacing ω . The numerical results for the metallic ($U = -0.7$, black circles) and superconducting ($U = -1.5$, red squares) regimes for $L = 700$ are indicated. The black (red dashed) line correspond to the GOE (GUE) distribution. Inset: The average level spacing $\langle \Delta_i^{N_A} \rangle$ as function of level number for both interactions.

the GOE distribution ($P_{\text{GOE}}(s) = (\pi s/2) \exp(-\pi s^2/4)$) expected for the excitations of interacting many particle systems [8, 9, 26–30]. On the other hand, in the superconducting regime the distribution follows the GUE distribution ($P_{\text{GUE}}(s) = (32s^2/\pi^2) \exp(-4s^2/\pi)$). Indeed, superconducting correlations lead to exotic statistics of the excitations close to the Fermi energy [32], which are quite similar to GUE for higher energies. Thus, also the ESLS distribution shows a significant difference between the metallic and superconducting phases, although for the length considered here ($L = 700 \ll \xi = 6 \cdot 10^5$) both regions are extended.

To conclude, the EE and ESLS distributions show a distinct behavior, depending if the system is in a metallic (system length much smaller than the localization length) or a superconducting (localization length diverges) regime, for a disordered one dimensional spinless electron system with attractive interactions. While the metallic regime shows a rather expected behavior, e.g., Gaussian distribution of the EE and GOE ESLS distribution, the superconducting EE shows an asymmetric distribution and GUE ESLS. Thus, the entanglement properties encode details of the underlying phase of the system which may elude other measures, which may be useful for detecting new phases for different systems. The emergence of a “fat tail” distribution for the EE in the superconducting regime is fascinating and deserves further study.

I would like to thank B. Altshuler, I. Aliener and V. Oganesyan, for useful discussions. Financial support from the Israel Science Foundation (Grant 686/10) is gratefully acknowledged.

-
- [1] For recent reviews see: L. Amico, R. Fazio, A. Osterloh, and V. Vedral, *Rev. Mod. Phys.* **80**, 517 (2008); J. Eisert, M. Cramer, and M. B. Plenio, *Rev. Mod. Phys.* **82**, 277 (2010); and references therein.
- [2] H. F. Song, S. Rachel, C. Flindt, I. Klich, N. Laflorencie, and K. Le Hur, *Phys. Rev. B* **85**, 035409 (2012).
- [3] H. Li and F. D. M. Haldane, *Phys. Rev. Lett.* **101**, 010504 (2008).
- [4] C. Holzhey, F. Larsen, and F. Wilczek, *Nucl. Phys. B* **424**, 443 (1994).
- [5] G. Vidal, J. I. Latorre, E. Rico, and A. Kitaev, *Phys. Rev. Lett.* **90**, 227902 (2003); J. I. Latorre, E. Rico, and G. Vidal, *Quant. Inf. Comp.* **4**, 048 (2004).
- [6] P. Calabrese and J. Cardy, *J. Stat. Mech.: Theor. Exp.* P06002 (2004).
- [7] V. E. Korepin, *Phys. Rev. Lett.* **92** 096402 (2004).
- [8] E. Prodan, T. L. Hughes, and B. A. Bernevig, *Phys. Rev. Lett.* **105**, 115501 (2010).
- [9] M. J. Gilbert, B. A. Bernevig, and T. L. Hughes, *Phys. Rev. B* **86**, 041401(R) (2012).
- [10] X. Chen, B. Hsu, T. L. Hughes, and E. Fradkin, *Phys. Rev. B* **86**, 134201 (2012).
- [11] R. Berkovits, *Phys. Rev. Lett.* **108**, 176803 (2012).
- [12] I. Mondragon-Shem, M. Khan, and T. L. Hughes, *Phys. Rev. Lett.* **110**, 046806 (2013).
- [13] A. Zhao, R.-L. Chu, S.-Q. Shen, *Phys. Rev. B* **87**, 205140 (2013).
- [14] R. Berkovits, *Phys. Rev. B* **89** 205137 (2014).
- [15] M. Pouranvari and K. Yang, *Phys. Rev. B* **89**, 115104 (2014).
- [16] A. M. Goldsborough and R. A. Römer, arXiv:1503.02973.
- [17] W. Apel, *J. Phys. C* **15**, 1973 (1982); W. Apel and T. M. Rice, *Phys. Rev. B* **26**, 7063 (1982).
- [18] T. Giamarchi and H. J. Schulz, *Phys. Rev. B* **37**, 325 (1988).
- [19] C. L. Kane and M. P. A. Fisher *Phys. Rev. B* **56**, 15231 (1997).
- [20] I. V. Gornyi, A. D. Mirlin, and D. G. Polyakov, *Phys. Rev. B* **75**, 085421 (2007).
- [21] M. P. A. Fisher and L. I. Glazmann, *Transport in one-dimensional Luttinger liquid in Mesoscopic Transport Theory*, Eds. L. Sohn, L. P. Kouwenhoven and G. Schön, (Kluwer, Amsterdam, 1997) NATO ASI Series E - Vol. 345, pp. 331-373.
- [22] P. Schmitteckert, T. Schulze, C. Schuster, P. Schwab, and U. Eckern, *Phys. Rev. Lett.* **80**, 560 (1998); P. Schmitteckert, R. A. Jalabert, D. Weinmann, and J. L. Pichard, *Phys. Rev. Lett.* **81**, 2308 (1998).
- [23] C. Schuster, R. A. Römer, and M. Schreiber, *Phys. Rev. B* **65**, 115114 (2002).
- [24] J. M. Carter and A. MacKinnon, *Phys. Rev. B* **72**, 024208 (2005).
- [25] R. Berkovits, *Europhys. Lett.* **25**, 681 (1994).
- [26] R. Berkovits and Y. Avishai, *J. of Phys. Condens. Matter* **8**, 389 (1996).
- [27] M. Pascaud and G. Montambaux, *Ann. der Physik* **7**, 406 (1998).
- [28] R. Berkovits and B. I. Shklovskii, *J. Phys. Condens. Matter* **11**, 779 (1999).
- [29] P. H. Song, and D. L. Shepelyansky, *Phys. Rev. B* **61**, 15546 (2000).
- [30] V. Oganesyan and D. A. Huse, *Phys. Rev. B* **75**, 155111 (2007); V. Oganesyan, A. Pal, and D. A. Huse, *ibid.* **80**, 115104 (2009).
- [31] R. Berkovits, *J. Phys. Condens. Matter* **7**, 4105 (1995).
- [32] A. Altland and M. R. Zirnbauer, *Phys. Rev. B* **55**, 1142 (1997).
- [33] R. A. Römer and M. Schreiber, *Phys. Rev. Lett.* **78**, 515 (1997).
- [34] F. Woynarovich and H. P. Eckerle, *J. Phys. A* **20**, L97 (1987); C. J. Hamer, G. R. W. Quispel, and M. T. Batchelor, *ibid.* **20**, 5677 (1987).
- [35] T. Giamarchi, *Quantum Physics in One Dimension* (Oxford University Press, New York, 2003).
- [36] S. R. White, *Phys. Rev. Lett.* **69**, 2863 (1992); *Phys. Rev. B* **48**, 10345 (1993).
- [37] U. Schollwöck, *Rev. Mod. Phys.* **77**, 259 (2005); K. A. Hallberg, *Adv. Phys.* **55**, 477 (2006).
- [38] R. Berkovits, *J. Phys.: Conf. Ser.*, **376**, 012020 (2012).
- [39] K. Burnecki, A. Wylomańska, A. Beletskii, V. Gonchar, and A. Chechkin *Phys. Rev. E* **85**, 056711 (2012) and references therein.